

Management of Greenhouse Solar Harvesting at Low Latitudes: Impacts of Slope, Curvature and Symmetry of the Envelope

Rui Mao¹, Zilong Zhao ^{1*}, Wenjun Pan², Xinlei Wang ^{1*}

¹ Department of Agricultural and Biological Engineering, University of Illinois at Urbana-Champaign, Urbana, IL 61801, USA

² School of Architecture, Design and Planning, the University of Sydney, Sydney, NSW 2008, Australia

(Corresponding Author: xwang2@illinois.edu)

ABSTRACT

Using passive solar energy for heating and lighting, greenhouses can be maintained at significantly lower energy consumptions. The design of the geometry of greenhouses, on the other hand, serves as a crucial factor that determines the effectiveness of solar energy absorption and thermal insulation depending on different indoor thermal conditioning requirements. This study conducts an analytical study regarding the impacts of greenhouse geometry on the intake of solar radiation. When altering the slope, curve, symmetry and the transparency of the greenhouse envelope, the light transmittance and the solar accumulation are found to be significantly varied. The overheating issue in summer and evaluated under different greenhouse configurations. The results of this study can be used to optimize the design of traditional greenhouses in different climate regions.

Keywords: greenhouse, passive solar technology, envelope geometry, design optimization

NONMENCLATURE

Abbreviations	
ABD	Ground Albedo
ALT	Altitude, m
AST	Apparent Solar Time
DST	Daylight-Saving Time
EoT	Equation of Time
NoD	Number of Days
SC	Solar Constant
WRC	World Radiation Center
Symbols	
α	Thermal diffusivity (m^2/s)
β	Intersection angle ($^\circ$)
δ	Solar declination ($^\circ$)
ϵ	Hemispherical emittance of the ground surface ($^\circ$)

ϕ	Latitude ($^\circ$)
γ	Surface azimuth angle ($^\circ$)
θ	Solar incidence angle ($^\circ$)
τ	Atmospheric transmittance coefficient
ω	Hour angle ($^\circ$)
Variables	
a, k, B	Coefficients
f	Transmissivity (%)
G	Solar radiation intensity (W/m^2)
r	Correction factor
Subscripts	
ex	Extraterrestrial
b	Normal/Direct
d	Diffuse
i	Infiltrated/Inner
o	Outer
z	Vertical component (solar zenith)

1. INTRODUCTION

Building consumptions account for approximately 40% of the total energy consumption [1,2]. In the field of agriculture, greenhouses typically integrate passive solar energy utilization to enhance greenhouse efficiency while minimizing energy demands [3,4]. The design of a greenhouse' geometry is thus the key to the effectiveness of passive solar energy utilization, which dictates its ability to absorb solar radiation and provide thermal insulation, thereby influencing the indoor thermal conditions. Understanding how variations in design variables impact system performance is essential in all engineering aspects [5,6]. And in greenhouses, solar energy intake can also be altered by optimizing greenhouse design to meet diverse thermal conditioning requirements.

This study aims to explore the intricate relationship between greenhouse geometry and solar radiation intake through an analytical investigation. By

manipulating parameters such as slope, curve, symmetry, and transparency of the greenhouse envelope, the study examines how these alterations affect light transmittance and solar accumulation within the structure. Particularly, this study addresses the challenge of overheating during hot months, a critical issue that must be mitigated to ensure optimal crop growing conditions. Our innovative design is to optimize the inner light environment based on the understanding of impacts of cover dimension on solar infiltration: avoid the intense sunlight and keep the proper radiation for crop growth. By integrating this structural optimization, the feasibility of the existing cooling methods, including the featured evaporative wet wall [7], natural controlled ventilation [8,9], natural ventilation augmentation [10,11] climate battery [12,13], etc. may be further enhanced to mitigate the overheating problem.

2. METHOD

2.1 The Extraterrestrial Radiation, G_{ex}

G_{ex} is the extraterrestrial radiation incident on the plane normal to the radiation, yearly varying depending on the sun-earth distance, derived by Eq. 1 [1].

$$G_{ex} = SC \begin{pmatrix} 1.000110 \\ +0.034221 \cos(B) \\ +0.001280 \sin(B) \\ +0.00719 \cos(2B) + \\ 0.000077 \sin(2B) \end{pmatrix} \quad (1)$$

where, SC is the solar constant, defined as the unit energy from the sun to the earth, which is 1367 W/m² adopted by the World Radiation Center (WRC); B , in degree, is given by Eq. 2 with the number of day (NoD).

$$B = \frac{360}{365} (NoD - 1) \quad (2)$$

2.2 The Solar Incidence Angle, θ

The incidence angle of beam radiation on a surface, θ , can be derived by Eq. 3.

$$\begin{aligned} \cos(\theta) = & \sin(\delta) \sin(\phi) \cos(\beta) - \\ & \sin(\delta) \cos(\phi) \cos(\gamma) + \\ & \cos(\delta) \cos(\phi) \cos(\beta) \cos(\omega) + \\ & \cos(\delta) \sin(\phi) \sin(\beta) \cos(\gamma) \cos(\omega) \\ & \cos(\delta) \sin(\beta) \sin(\gamma) \sin(\omega) \end{aligned} \quad (3)$$

where, β is the slope between the surface and the horizon, γ is the surface azimuth angle, the deviation of the projection on a horizontal plane of the normal to the surface from the local meridian, due south zero, east negative, west positive; δ is the solar declination, the angular position of the sun at solar noon, north positive, south negative, based on Eq.4; ω is the hour angle, based on Eq. 5 [14].

$$\delta = \begin{pmatrix} 0.006918 \\ -0.399912 \cos(B) \\ +0.070257 \sin(B) \\ -0.006758 \cos(2B) \\ +0.000907 \sin(2B) \\ -0.002697 \cos(3B) \\ +0.00148 \sin(3B) \end{pmatrix} \left(\frac{180}{\pi} \right) \quad (4)$$

$$\omega = 15 \times (AST - 12) \quad (5)$$

where AST is the apparent solar time, in hour.

2.3 The Atmospheric Transparency

Weather fluctuations can significantly affect the solar radiation that goes through the atmosphere. There exists proved prediction models for atmospheric transparency [7]. Note that even under a clear atmospheric condition, the atmosphere still has an impact on the radiation reaching the ground. In this study, the radiation is formulated as a function of atmospheric transmittance, as defined, and shown by Eqs. (6.1-6.2). τ_b is a function of the solar zenith, θ_z , and τ_d can be derived based on τ_b , as presented by Eqs. (7.1-7.2) [15]. According to the specific altitude and climate, the correction parameters of τ_b can be applied as shown in Eq. (8.1-8.3) and the coefficients are listed in Tab. 2. θ_z can be derived by Eq. (3) with β is zero.

$$G_b = G_{ex} \tau_b \quad (6.1)$$

$$G_d = G_{ex} \cos(\theta_z) \tau_d \quad (6.2)$$

$$\tau_b = a_0 + a_1 \exp\left(-\frac{k}{-\cos(\theta_z)}\right) \quad (7.1)$$

$$\tau_d = 0.271 - 0.294 \tau_b \quad (7.2)$$

$$a_0 = r_0 [0.4237 - 0.00821(6 - ALT)^2] \quad (8.1)$$

$$a_1 = r_1 [0.5055 + 0.00595(6.5 - ALT)^2] \quad (8.2)$$

$$k = r_k [0.2711 + 0.01858(2.5 - ALT)^2] \quad (8.3)$$

Tab. 1 Correction factors in the calculation of atmospheric transparency

Climate Type	r_0	r_1	r_k
Tropical	0.95	0.98	1.02
Mid-latitude summer	0.97	0.99	1.02
Subarctic summer	0.99	0.99	1.01
Mid-latitude winter	1.03	1.01	1.00

2.4 The Clear-Sky Solar Irradiance Incidence on Receiving Surface

The total solar irradiance reaching the receiving surface, G_t , can then be obtained by combining three components—the beam radiance $G_{t,b}$, the reflected radiance $G_{t,r}$, and the diffuse radiance $G_{t,d}$, as shown by Eq. (9). The further derivations for these three components are presented by Eqs. (10.1-10.3).

$$G_t = G_{t,b} + G_{t,d} + G_{t,r} \quad (9)$$

$$G_{t,b} = G_b \cos(\theta) \quad (10.1)$$

$$G_{t,r} = (G_b \cos(\theta_z) + G_d) ABD \left(1 - \frac{\cos(\beta)}{2}\right) \quad (10.2)$$

$$G_{t,d} = G_d \left[\frac{AI \times R_b + (1 - AI) \frac{(1 + \cos(\beta))}{2}}{1 + \sqrt{\frac{G_b}{G_b \cos(\theta_z) + G_d} \sin^3\left(\frac{\beta}{2}\right)}} \right] \quad (10.3)$$

where ABD denotes the ground albedo (or hemispherical reflectance), expressed as a fraction between 0 and 1. An albedo of 1 implies that all sunlight is reflected without absorption, whereas an albedo of 0 means that all sunlight is absorbed. The commonly used albedo values for different surfaces can be found in the documented studies [16]. In this study, NASA monthly global albedo map was used to determine the value of ground albedo [17]. The diffuse radiation, $G_{t,d}$, can be formulated using Hay-and-Davies model, further modified by adding a horizon brightening, which is shown by Eq. (13), where AI denotes the anisotropy index, which is defined as G_d/G_{ex} and R_b is the geometric factor which equals to $\cos(\theta)/\cos(\theta_z)$ [18, 19]. Known as HDKR model, it is simpler to use while still maintaining a high accuracy.

2.5 Cover Light Infiltration

There are two key variables related to glass and film infiltration—the infiltration angle and the coating optical property. There is an experimental relationship between the transmissivity, f , and the incidence angle, θ , as shown in Eq. (11) and Fig. 1 ($a=1$ in the reference), which indicates the perpendicular incidence has the highest cover infiltration [20]. When the incident angle reaches beyond 40° , light transmission through the glass would experience a sharp decrease, and when beyond 80° , most light would be reflected instead of being transmitted [21].

$$f_i = (f_i)_{max} \left(1 - a \left(\frac{\theta}{90}\right)^4\right) \quad (11)$$

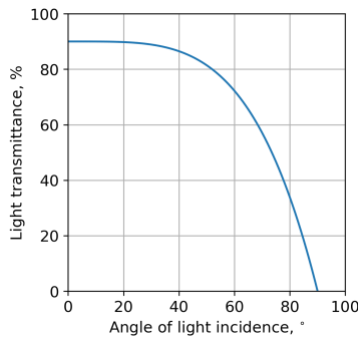


Fig. 1 Plot of light transmittance VS angle of light incidence.

Then, for a single-slope greenhouse, we can roughly estimate the infiltrated solar radiation, G_i , by Eq. (12).

$$G_i = G_o f_i \quad (12)$$

3. RESULTS

Fig. 2 demonstrates the potential variations that can be achieved on the geometry of greenhouse through the perspectives of inclination, symmetry, and curvature.

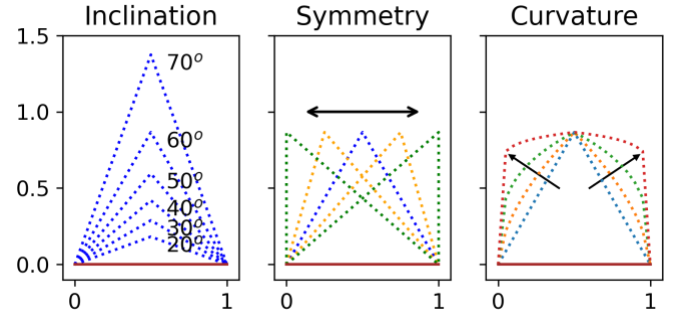


Fig. 2 Geometric characteristics of greenhouses

3.1 Inclination

In this study, the study range of the roof inclination is from 20° to 70° . And the latitude range is concentrated between 0°N to 40°N . In Fig. 4, five varied, representative latitudes 0°N , 10°N , 20°N , 30°N , and 40°N and multiple magnitudes of slopes are selected to show the impacts of slopes on the total solar energy accumulation in the greenhouse.

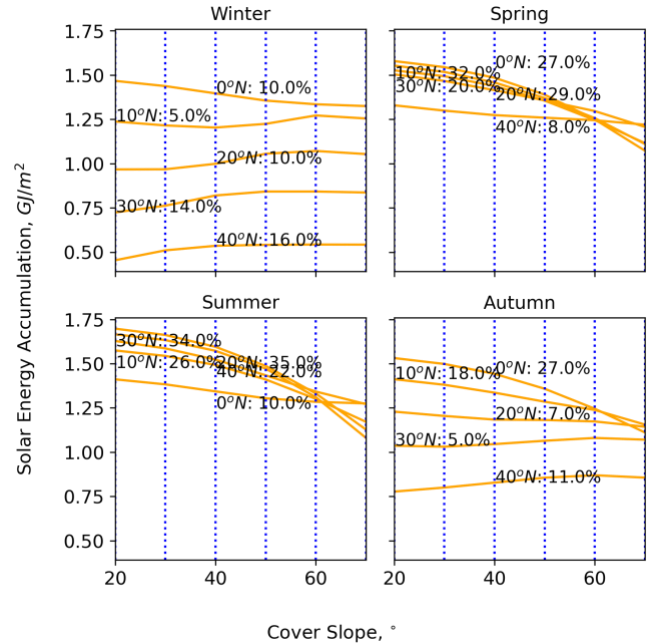


Fig. 3 Impacts of slopes and latitudes on solar accumulation.

It can be observed that the significance of slope variation is exhibited most prominently in spring and summer. For instance, in spring, when the latitude is 20°N , and when the slope increases from 20° to 70° , the solar accumulation decreases by 29% from 1.55 to 1.11

GJ/m². In general, the solar accumulation is negatively changing with the increase in slope, except for winter. In winter, the same trend can only be found near the equatorial region, and in most cases, the greenhouses can obtain more solar energy when the slope increases. Therefore, to sum it up, when it comes to lower latitude (close to 0°N), to mitigate the overheating issue in summer and enhance the management of solar energy harvesting, it is recommended to use steeper slopes. On the other hand, when it comes to higher latitude (close to 40°N), though the steeper slopes may slightly increase the solar absorption in greenhouse in cold seasons, of which the impacts to the annual greenhouse performance are minor, the steeper slopes should still be recommended.

3.2 Symmetry

As Fig. 2 (Symmetry), we set the symmetry variation, keeping the same overall height, moving the apex from the front side to the back side by an interval of ¼ cross-sectional width. The study of the effects of geometric symmetry is conducted over all latitudes from 0 to 40°N. Here we present the results for 20°N.

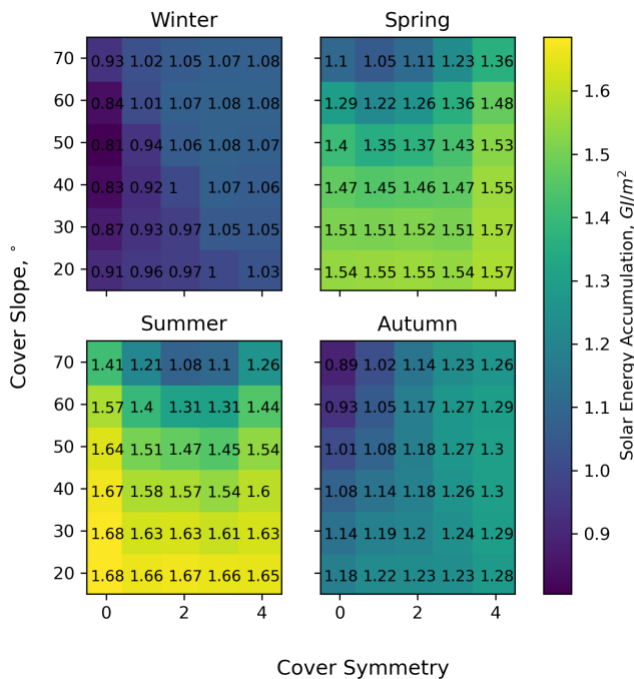


Fig. 4 Coupling effects of slopes and symmetry on solar accumulation.

From Fig. 4, the influence of symmetry is more significant during autumn and winter seasons, where a steeper roof inclination towards the front results in less accumulation of sunlight. Conversely, during spring and summer, the roof angle has a larger impact, with steeper roofs accumulating less sunlight. Considering winter and summer separately, selecting a symmetrical roof with a

large angle ensures minimal sunlight exposure during summer, while still maintaining moderate sunlight accumulation during winter. According to systematic research, the effects of changing symmetry vary depending on latitude. Near the equator, when the roof is positioned further back, there is less sunlight accumulation during spring and summer; whereas, when the roof is positioned further forward, there is less sunlight accumulation during autumn and winter. This is because sunlight is abundant throughout the year, requiring further balancing of symmetry.

In higher latitude regions, when the roof is positioned further forward, there is less sunlight accumulation during spring and summer; whereas, when the roof is positioned further back, there is less sunlight accumulation during autumn and winter. Therefore, selecting a larger roof angle with a forward inclination ensures less sunlight exposure during spring and summer, while maintaining moderate sunlight exposure during autumn and winter. Overall, roofs with larger angles of symmetry (or forward inclination) can optimize the solar greenhouse effect in temperate climates.

3.3 Curvature

In the study of curvature, the greenhouse symmetry is maintained constant. First, on the rear roof surface, no curvature is set and the curvature changes on the front roof surface is observed. Then, the straight slope is applied to the front roof surface and the curvature changes on the rear roof surface are conducted.

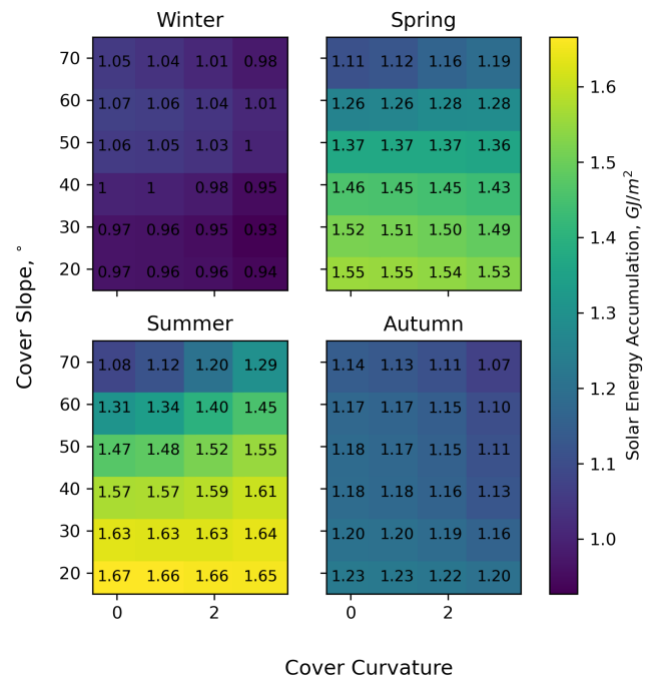


Fig. 5 At latitude of 20°N, the impacts of curvature on the front roof on solar accumulation.

It can be observed that during spring and summer, roofs without a flat or steep inclination are able to maintain a lower amount of sunlight, while during winter, there is a moderate amount of sunlight that can be allowed.

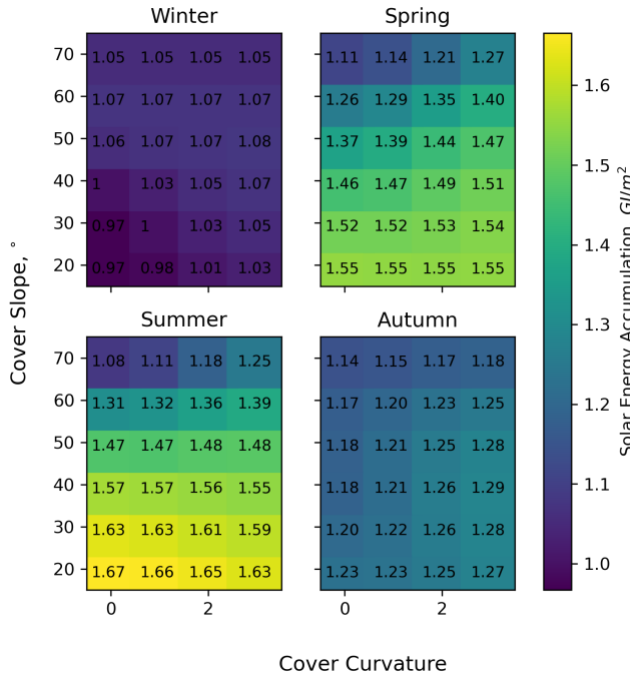


Fig. 6 At latitude of 20°N, the impacts of curvature on the rear roof on solar accumulation.

It can be observed that the trends during spring and summer are generally consistent regarding the effects of curvature variations at the front roof. For autumn and winter, although the effects of curvature changes are opposite, for example, during winter, increasing curvature on the front roof surface decreases sunlight accumulation, while increasing curvature on the rear roof surface increases sunlight accumulation, if set to a large angle roof, the impact of curvature diminishes. Overall, a large-angle roof with minimal curvature is more suitable.

4. DISCUSSIONS BASED ON THE RESULTS

For specific regions, the optimal combination of angle/symmetry/curvature can be achieved through detailed model calculations. However, a more general optimization concept can now be concluded as flat or steep symmetrical roofs can effectively reduce sunlight accumulation. The angle of the roof slope has the greatest impact, while symmetry and curvature can be appropriately fine-tuned according to overall requirements case-by-case [22].

On the other hand, steep slopes can affect space utilization. In the overall design of the greenhouse roof, if there are steep sections of slopes, there must be flatter

sections. Therefore, it could be wise to allow sunlight to pass through the steep sections of the roof while making the flatter sections, which receive ample sunlight, opaque to maximize structural efficiency.

The resulting design features transparent sections on the front-facing steep roof and opaque sections on the flatter areas on top, as illustrated in the diagram.

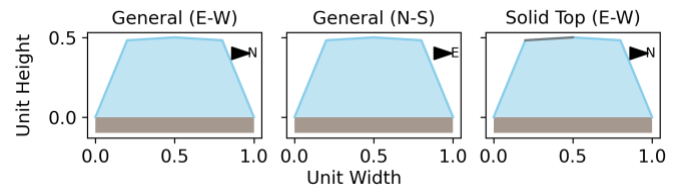


Fig. 7 At latitude of 20°N, the impacts curvature on the rear roof on solar accumulation.

Tab. 2 Solar Accumulation at 20°N, 61° front slope, and 16° top slope.

Solar Accumulation GJ/m ²	General (E-W)	General (N-S)	Solid Top (E-W)
Winter	0.54	0.17	0.49
Spring	1.31	1.36	0.84
Summer	1.51	1.87	0.98
Autumn	0.86	0.52	0.61
Full Year	4.23	3.92	2.92

Here, we compared the traditional fully transparent greenhouse setup, both in north-south and east-west orientations, with the new design's targeted performance in the north-south orientation. Adjusting greenhouse orientation from east-west to north-south in warmer regions exhibits reduction in overall sunlight accumulation yet fails to address excessive radiation in spring and summer while reducing sunlight in autumn and winter. Conversely, maintaining an east-west orientation with a sloped roof can better control sunlight exposure in spring and summer while minimizing reductions in autumn and winter, ensuring more uniform radiation distribution year-round.

5. CONCLUSIONS

In this paper, a theoretical analysis is conducted on the influence of greenhouse geometry on solar at low latitudes. The main conclusions can be drawn below.

- By adjusting the roof slope, the solar accumulation can be significantly altered, particularly during high-temperature seasons, by up to 40%.
- Maintaining constant height while adjusting symmetry also affects solar accumulation but shows limited impacts.

- c) When the height and symmetry of the roof are constant, the variations in the roof curvature may affect the solar accumulation by over 19%.

Overall, through comparison, it was found that this design could better block excessive solar radiation while allowing sufficient sunlight by optimizing the geometric design of the greenhouse.

REFERENCE

- [1] Z. Zhao, Y. Lin, A. Stumpf, and X. Wang. 2023. Improving LEED-certified building loads on borehole heat exchangers by coupling subsurface variables. *Appl. Therm. Eng.* 224, 120119. <https://doi.org/10.1016/j.applthermaleng.2023.120119>
- [2] Z. Zhao, A. Stumpf, Y. Lin, and X. Wang. 2022. Impacts of prospective LEED building's energy loads on a borehole heat exchanger: A case study in Central Illinois. *Proceedings of the IGSHA Research Track*. <http://dx.doi.org/10.22488/okstate.22.000030>
- [3] R. Mao, Z. Zhao, L. Tian, T. Fang, and X. Wang. 2023. Generation of gridded temperature map of constant-temperature layer based on meteorological data for shallow geothermal applications. *Geothermics*. 113 102770. <https://doi.org/10.1016/j.geothermics.2023.102770>.
- [4] Z. Zhao, Y. Lin, A. Stumpf, and X. Wang. 2022. Assessing impacts of groundwater on geothermal heat exchangers: A review of methodology and modeling. *Renew. Energy*. 190, 121-147. <https://doi.org/10.1016/j.renene.2022.03.089>
- [5] Z. Zhao, G. Lv, Y. Xu, Y. Lin, P. Wang, and X. Wang. 2024. A Stochastic Optimization Model for a Ground Source Heat Pump System with Uncertainty Quantifications on Transient Geologic Variables. *Stanford University*. SGP-TR-227.
- [6] Z. Zhao, Y. Xu, Y. Lin, X. Wang and P. Wang. 2021. Probabilistic modeling and reliability-based design optimization of a ground source heat pump system. *Appl. Therm. Eng.* 197, 117341. <https://doi.org/10.1016/j.applthermaleng.2021.117341>
- [7] K. Hull, M. Mabitsela, E. Phiri, and M. J. Booyens. 2023. Dataset of temperature, humidity, and actuator states of an east-facing south African greenhouse tunnel. <https://doi.org/10.2139/ssrn.4560827>
- [8] L. O. Chahidi and A. Mechaqrane. 2023. Energy and economic analysis for the selection of optimal greenhouse design: A case study of the six Morocco's climatic zones. *Energy Build.* 289, 113060 (June 2023), 113060.
- [9] *Study of a novel front- roof-back natural ventilation system for Chinese solar greenhouses.*
- [10] L. McCartney and M. G. Lefsrud. 2018. Field trials of the Natural Ventilation Augmented Cooling (NVAC) greenhouse. *Biosyst. Eng.* 174, (October 2018), 159–172.
- [11] L. McCartney, V. Orsat, and M. G. Lefsrud. 2018. An experimental study of the cooling performance and airflow patterns in a model Natural Ventilation Augmented Cooling (NVAC) greenhouse. *Biosyst. Eng.* 174, (October 2018), 173–189. <https://doi.org/10.1016/j.biosystemseng.2018.07.005> <https://doi.org/10.1016/j.enbuild.2023.113060>
- [12] K. H. Lee and R. K. Strand. 2008. The cooling and heating potential of an earth tube system in buildings. *Energy Build.* 40, 4 (January 2008), 486–494. <https://doi.org/10.1016/j.enbuild.2007.04.003>
- [13] R. Mao, Z. Zhao, L. Tian, X. Wang and R. Maghirang. 2024. Mapping the Distribution of the Neutral Zone in Assist of Shallow Geothermal Applications in the United States. *Stanford University*. SGP-TR-227.
- [14] M. Iqbal. 1983. Solar radiation incident on tilted planes on the earth's surface. In *An Introduction to Solar Radiation*. Elsevier, 303–334. <https://doi.org/10.1016/b978-0-12-373750-2.50016-1>
- [15] B. Y. H. Liu and R. C. Jordan. 1960. The interrelationship and characteristic distribution of direct, diffuse and total solar radiation. *Sol. Energy* 4, 3 (July 1960), 1–19. [https://doi.org/10.1016/0038-092x\(60\)90062-1](https://doi.org/10.1016/0038-092x(60)90062-1) <https://doi.org/10.1016/j.biosystemseng.2018.07.004>
- [16] D. Thevenard and K. Haddad. 2006. Ground reflectivity in the context of building energy simulation. *Energy Build.* 38, 8 (August 2006), 972–980. <https://doi.org/10.1016/j.enbuild.2005.11.007>
- [17] MODIS/Terra Land Surface Temperature/Emissivity Monthly L3 Global 0.05Deg CMG V006.
- [18] T. M. Klucher. 1979. Evaluation of models to predict insolation on tilted surfaces. *Sol. Energy* 23, 2 (1979), 111–114. [https://doi.org/10.1016/0038-092x\(79\)90110-5](https://doi.org/10.1016/0038-092x(79)90110-5)
- [19] D. T. Reindl, W. A. Beckman, and J. A. Duffie. 1990. Evaluation of hourly tilted surface radiation models. *Sol. Energy* 45, 1 (1990), 9–17. [https://doi.org/10.1016/0038-092x\(90\)90061-g](https://doi.org/10.1016/0038-092x(90)90061-g)
- [20] W. Xuan. 2006. Mathematical model establishment and analysis for greenhouse surface curve (in Chinese). *Tianjin Agricultural Scien* 12, 4 (2006), 44–46.
- [21] W. C. Lawrence. 1950. *Science and the glasshouse*. Oliver & Boyd, Edinburgh, G.B.
- [22] S. Gorjian, et al. 2021. A review on opportunities for implementation of solar energy technologies in agricultural greenhouses. *J. Clean. Prod.* 285 (20) 124807. <https://doi.org/10.1016/j.jclepro.2020.124807>